Observation of Synchronization in Laser Chaos

Toshiki Sugawara,* Maki Tachikawa, Takayuki Tsukamoto, and Tadao Shimizu†
Department of Physics, Faculty of Science, University of Tokyo, 7-3-1 Hongo, Bunkyo-ku, Tokyo 113, Japan
(Received 9 November 1993)

We experimentally demonstrate that two chaotic passive Q-switched lasers can be synchronized by modulating the saturable absorber in the cavity of one laser with the output of the other laser. The entrainment of the chaotic motion takes place when the slave system has a slightly different strange attractor from that of the master system. The observed synchronized pulsation of the two lasers is well reproduced by the computer simulation based on our rate-equation model.

PACS numbers: 42.50.Ne

In a chaotic system, a distance between two close points in the phase space is extended with time. This generic nature of chaos seems to prevent synchronization of chaotic motions of two systems even though the fundamental equations are perfectly identical. Recently, however, synchronization of chaos has been revealed to take place spontaneously in several physical systems such as electric circuits [1]. Moreover, it may bring many interesting possibilities in practical applications in the fields of neural networks [2] and communications [3].

Pecora and Carroll [1] demonstrated that two identical chaotic systems (master and slave systems) can be made to synchronize by linking them with a common signal. In their strategy, certain variables of the slave system are replaced by those of the master system so that the master system can drive a part of the slave system. The synchronization between the two systems occurs, critically depending on the sign of the sub-Lyapunov exponents.

On the other hand, in locally coupled nonlinear oscillators, chaotic outputs from different units are observed to synchronize under certain conditions. In this case, the synchronization is mutual in the sense that the subsystems affect each other and they cannot be identified as a master or a slave component. This phenomenon is theoretically predicted in optical systems, such as coupled diode laser arrays [4] and coupled ring cavities with nonlinear media [5].

Although synchronized chaos is realized in various theoretical models, few experimental evidences in real systems have been demonstrated so far. In this Letter, we report experimental observation of synchronization of optical chaos for the first time to our knowledge. Here we consider the situation where one chaotic laser is driven by the output of another chaotic laser. Our system consists of two CO_2 lasers with gaseous saturable absorbers; one is the master laser and the other is the slave laser. A saturable absorber inside the laser cavity induces self-sustained pulsation in a single-mode oscillation which is known as passive Q switching (PQS). In the case of the CO_2 laser, the chaotic passive Q-switching pulsation appears after the period-doubling bifurcation [6]. It is demonstrated that the two chaotic PQS pulsations are synchronized when the radiation from the master laser is injected into the saturable absorber of the slave laser. The laser system is designed so that the slave laser radiation is not fed into the master laser. There is no reaction force acting back to the driving system.

Experimental setup of the laser system is shown in Fig. 1. The master and slave CO_2 lasers, respectively, consist of 2.1 m and 1.5 m long discharge gain tubes and 35 cm and 48 cm long intracavity absorption cells which are sealed by Brewster windows. The infrared radiation of the two lasers is polarized linearly in the direction parallel to each other. Total cavity length is 3.5 m for the master laser and 2.6 m for the slave laser. Both lasers oscillate in a single TEM_{00} mode of the 10 μm $R(28)$ line.

Gas mixture of CO_2, N_2, and He is flowing through the gain tubes. The total pressure and the mixing ratio are 7.1 Torr and 1.0:0.9:7.0 in the master laser, and 8.0 Torr and 1.0:3.2:8.5 in the slave laser. SF_6 is introduced into the absorption cell as a saturable absorber, and CH_3OH or He is added to the absorber as a buffer gas. In the master laser, the pressure of SF_6 is 15 mTorr and that of the CH_3OH buffer gas is 145 mTorr, while the pressure of SF_6 is 17 mTorr and that of the He buffer gas is 96 mTorr in the slave laser.

The output beam of the master laser is injected into the absorption cell of the slave laser through the antireflection (AR)-coated ZnSe window after its polarization is rotated by 90° with the mirror system. The injected beam is focused on the center region of the cell by a lens with a focal length of 25.4 cm. The power of the incident beam is adjustable by changing the aperture of the iris placed on the light path. The incident beam is overlapped with the radiation of the slave laser between the

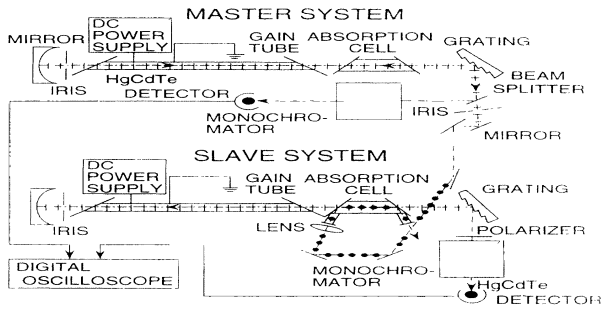

FIG. 1. Diagram of the experimental setup.

0031-9007/94/72(22)/3502(4)$06.00

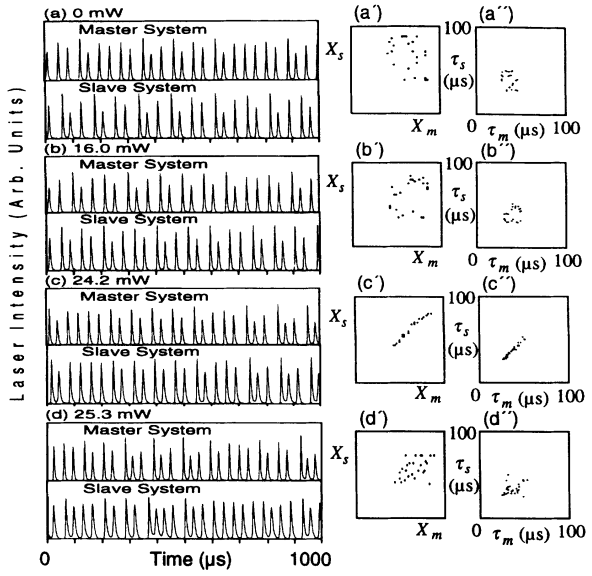

FIG. 2. Observed time sequences of the PQS pulsation of the master and slave lasers for different powers of the injected beam [(a)-(d)] together with the correlation plots between the peak heights [(a')-(d')] and between the peak intervals [(a")-(d")].

two Brewster windows of the absorption cell, and then comes out of the other AR-coated window. The power reflectivity of the Brewster window for the polarization component perpendicular to the plane of incidence is estimated to be 50%. The output beam of the slave laser is superposed by the master laser beam transmitted into the slave laser's cavity through one end of the absorption cell. The master laser beam is cut off by the polarizer placed before the detector.

Figures 2(a)-2(d) show time sequences of the PQS pulsations from the two lasers for different values of the input power of the master laser beam. To examine the correlation in the amplitude between the two signals, the intensity of the peak in the slave laser output X_s is plotted against that of the peak in the master laser output X_m which has appeared just before it [Figs. 2(a')-2(d')]. Simultaneously, the correlation in the phase of the chaotic motions is investigated as follows. The time interval between the nth peak and the next peak in the slave laser output is denoted by $\tau_{s,n}$. $\tau_{s,n}$ is plotted in Figs. 2(a")-2(d") as a function of the time interval between two adjacent peaks in the master laser output, $\tau_{m,n}$, the former of which has appeared just before the nth peak of the slave laser output. If the two lasers are synchronized, X_s and τ_s are linearly dependent on X_m and τ_m, respectively.

When there is no coupling between the two systems, each laser exhibits chaotic pulsations as shown in Fig. 2(a). In the X_s-X_m and τ_s-τ_m plots, data points are scattered two dimensionally in an erratic manner, indicating that the two lasers are pulsating independently. The two

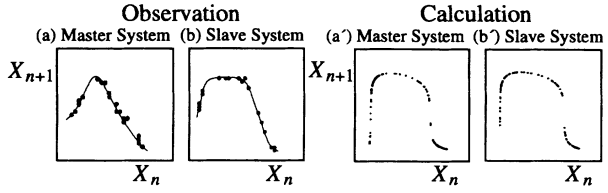

FIG. 3. Lorenz plots of the chaotic PQS pulsations of the two lasers when they are operated independently.

pulsations remain little correlated at the input power of 16.0 mW. When the input power is raised up to 24.2 mW, the chaotic pulsation of the slave laser is synchronized to the driving pulsation as seen in Fig. 2(c). A linearity is clearly observed in the relations of the corresponding peak heights and intervals, although the data points slightly deviate from the straight lines because of the presence of external noise. The cross correlation analysis reveals that the response of the slave laser is delayed from the driving pulsation roughly by 9 μs. When the input power is further increased to 25.3 mW, the synchronization is destroyed as is shown in Fig. 2(d).

The synchronization is realized between two chaotic systems which settle on slightly different strange attractors without couplings. Figure 3 shows the first return map (or the Lorenz plot) constructed from the observed time series. The Lorenz plot provides correlation between adjacent peak heights of the time sequence, X_{n+1} vs X_n, and corresponds to a cross section of the attractor on a specific plane in the phase space. When the lasers are operated independently, the Lorenz plot of both lasers traces a nearly one-dimensional curve shown in Figs. 3(a) and 3(b). Their detailed shapes are different because of the discrepancy in the system parameters; that is, the master laser has a unimodal plot with an acute peak, while the Lorenz plot of the slave laser exhibits a relatively flat top.

We carry out a rate-equation analysis to reproduce the observed dynamics of the coupled CO_2 laser system. According to the three-level-two-level model, which was successfully employed to analyze the PQS dynamics in our previous publications [6-8], the present laser system is described by the following rate equations for the normalized photon density I, population density in the upper laser level M_1, population density in the lower laser level M_2, and difference of the population density in the absorber levels N:

$$dI_m/dt = [(M_{1,m} - M_{2,m}) - B_m N_m - k_m] I_m ,$$

$$dM_{1,m}/dt = P_m M_m - R_{10,m} M_{1,m} - (M_{1,m} - M_{2,m}) I_m ,$$

$$dM_{2,m}/dt = -R_{20,m} M_{2,m} + (M_{1,m} - M_{2,m}) I_m ,$$

$$dN_m/dt = -2 b_m N_m I_m - r_m (N_m - 1) ,$$

$$dI_s/dt = [(M_{1,s} - M_{2,s}) - B_s N_s - k_s] I_s ,$$

$$dM_{1,s}/dt = P_s M_s - R_{10,s} M_{1,s} - (M_{1,s} - M_{2,s}) I_s ,$$

TABLE I. Notation of the parameters in the equations.

Parameter	Description
B	Normalized rate of absorption in the loss medium.
k	Cavity loss rate.
P	Rate of the pumping to the upper laser level.
M	Population density of CO_2 in the ground level.
R_{10}	Rate of the vibrational relaxation from the upper laser level to all other levels except the lower laser level.
R_{20}	Rate of the vibrational relaxation from the lower laser level to all other levels except the upper laser level.
b	Normalized cross section of the absorption in the loss medium.
r	Rotational relaxation rate of the absorptive levels.
C	Coupling coefficient ($0 \le C \le 1$).

$$dM_{2,s}/dt = -R_{20,s}M_{2,s} + (M_{1,s} - M_{2,s})I_s ,$$

$$dN_s/dt = -2b_sN_s(I_s + CI_m) - r_s(N_s - 1) .$$

Here the subscripts m and s refer to the variables and parameters of the master and slave laser systems, respectively. The notations of the parameters are summarized in Table I. Detailed formulation of the rate equations and a procedure of the normalization of the variables are described elsewhere [8]. The radiation of the master laser modulates the absorber's population in the slave laser through the second term on the right side of the last equation, where C is a coupling coefficient. Part of the injected beam is transmitted into the gain tube through the Brewster windows. However, its effect on the population of CO_2 is negligible because (1) its intensity is considerably weaker than in the absorption cell due to the reflection at the windows and the divergence after the focusing, and (2) the saturability of the gain medium is much smaller than the absorber. The parameter values used in the numerical integration appear in Table II. They are reasonable for the present CO_2 lasers. For simplicity, the parameter values of the two systems are assumed identical except the pumping rate.

The observed dependence of the chaotic PQS pulsations on the strength of the driving force is qualitatively reproduced by the computer simulation. Figure 4 shows calculated time sequences of the photon density and the X_s-X_m and τ_s-τ_m plots as functions of the coupling coefficient. When $C=0$, the master and slave lasers produce chaotic pulsations characterized by the Lorenz plots in Figs. 3(a') and 3(b'), respectively. The two lasers settle on the strange attractors slightly different from each other; that is, the Lorenz plot of the slave laser chaos has a shorter tail than that of the master laser chaos on the left side of the unimodal curve. The photon density of the slave laser is synchronized to the driving pulsation at the coupling coefficient of 5.33% that is consistent with the input power where the synchronization is experimentally

TABLE II. Parameter values used in the analysis.

Parameter	m: Master system	s: Slave system
B (MHz)	1.5	1.5
k (MHz)	2.0	2.0
P (Hz)	16.70	16.45
M (MHz)	3820	3820
R_{10} (MHz)	0.0003	0.0003
R_{20} (MHz)	0.38	0.38
b	900.0	900.0
r (MHz)	6.0	6.0

observed. The delay of 3 μs is observed between the two pulsations, which qualitatively agrees with the experimental result. The synchronization breaks at a larger or smaller coupling coefficient.

The variance of the X_s-X_m plot from the best-fitted linear relation, $\sigma^2 = (1/N)\sum_i^N (X_{s,i} - aX_{m,i})^2$, is measured for $N=100$ data points sampled from the calculated time sequences. The peak values are normalized to the maximum in each time sequence. Figure 5(a) shows the variance as a function of the coupling coefficient when P_s is 16.45 Hz. Synchronization occurs in a limited parameter range around $C=4\%$. Under the best conditions for the coupling, the variance is reduced by almost 3 orders of magnitude from the uncorrelated state at $C=0$. The parameter region where the variance falls below 0.008 is shown in the phase diagram for P_s and C in Fig. 5(b). Synchronization occurs only when P_s is smaller than P_m. Net gain of the slave laser is increased by the injected beam since it contributes to the saturation of the loss

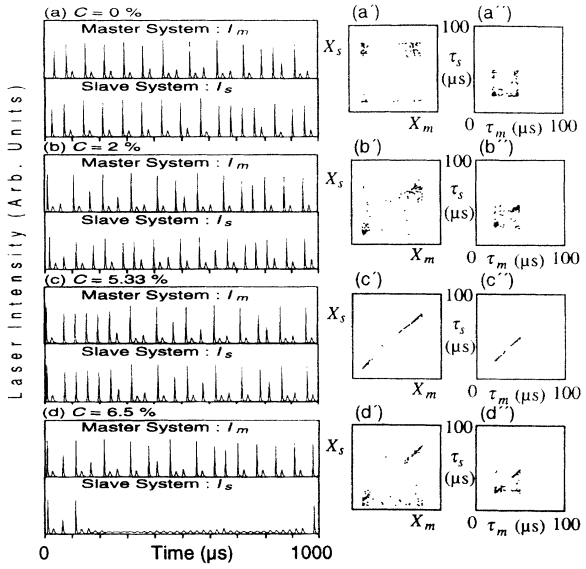

FIG. 4. Calculated time sequences of the PQS pulsation of the master and slave lasers for different coupling coefficients [(a)-(d)] together with the correlation plots between the peak heights [(a')-(d')] and between the peak intervals [(a'')-(d'')].

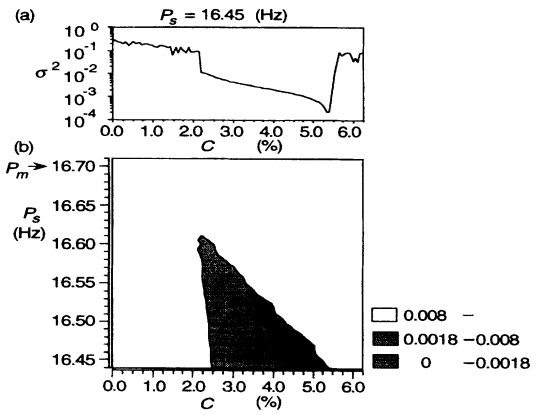

FIG. 5. (a) Variance of the X_s-X_m plot from the best-fitted linear relation $X_s = aX_m$ as a function of the coupling coefficient C. The variance is measured for 100 data points sampled from the time series calculated at $P_s = 16.45$ Hz. (b) Contour lines of the variance over the parameter space for P_s and C.

medium of the slave laser. The injection has the same effect as raising the excitation strength. In order for the slave system under the influence of the injection to settle on the same attractor as the master system, it is necessary that its excitation level be set lower than the master system.

The synchronized PQS pulsation is a chaos version of the frequency entrainment generally known as an effect in a periodically driven oscillator. In an ordinary entrainment, the driven system gives up its independent mode of oscillation and acquires the frequency of the applied periodic force. The attractor of the driven system is transformed to a limit cycle that is synchronized to the driving force as its influence becomes dominant. Our observation demonstrates that the entrainment may take place even when the driving force is chaotic if it is based on a strange attractor nearly identical with the intrinsic one of the slave system.

In conclusion, chaotic PQS pulsations of two CO_2 lasers have been demonstrated both experimentally and theoretically to be made to synchronize by injecting the output beam from one laser to the saturable absorber of the other laser. The present system differs from Pecora and Carroll's regime in that the slave system shares no degrees of freedom with the master system. We believe that the phenomenon of the chaotic entrainment may generally occur in externally driven nonlinear systems. Detailed mechanism of the synchronization, such as the major factor to determine the delay time between the two outputs, is currently being investigated and will be reported soon.

We gratefully acknowledge Dr. T. Tohei, Science University of Tokyo, for his aid in the numerical calculation. We wish to thank S. Otuka and M. Hirano for constructing parts of the CO_2 laser apparatus.

*Present address: Central Research Laboratory, Hitachi Ltd., 1-280 Higashikoigakubo, Kokubunji-City, Tokyo-185, Japan.

†Present address: Department of Physics, Science University of Tokyo, 1-3 Kagurazaka, Shinjuku-ku, Tokyo-162, Japan.

[1] L. M. Pecora and T. L. Carroll, Phys. Rev. Lett. **64**, 821 (1990).

[2] J. M. Kowalski *et al.*, Neural Networks **5**, 805 (1992).

[3] S. Hayes, C. Grebogi, and E. Ott, Phys. Rev. Lett. **70**, 3031 (1993).

[4] H. G. Winful and L. Rahman, Phys. Rev. Lett. **65**, 1575 (1990).

[5] Jyh-Long Chern and John K. McIver, Phys. Lett. A **151**, 150 (1990).

[6] M. Tachikawa *et al.*, Phys. Rev. Lett. **60**, 2266 (1988).

[7] M. Tachikawa, K. Tanii, and T. Shimizu, J. Opt. Soc. Am. B **5**, 1077 (1988).

[8] M. Tachikawa, K. Tanii, and T. Shimizu, J. Opt. Soc. Am. B **4**, 387 (1987).

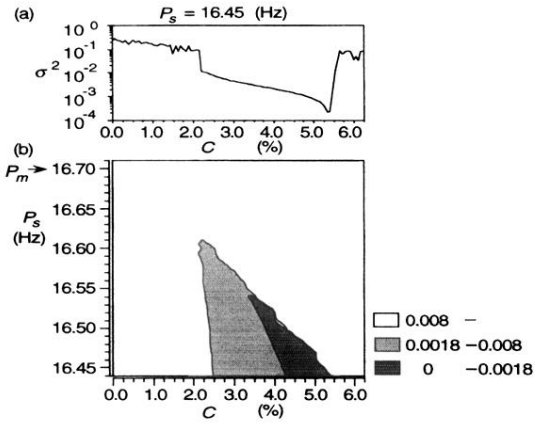

FIG. 5. (a) Variance of the X_s-X_m plot from the best-fitted linear relation $X_s = aX_m$ as a function of the coupling coefficient C. The variance is measured for 100 data points sampled from the time series calculated at $P_s = 16.45$ Hz. (b) Contour lines of the variance over the parameter space for P_s and C.